

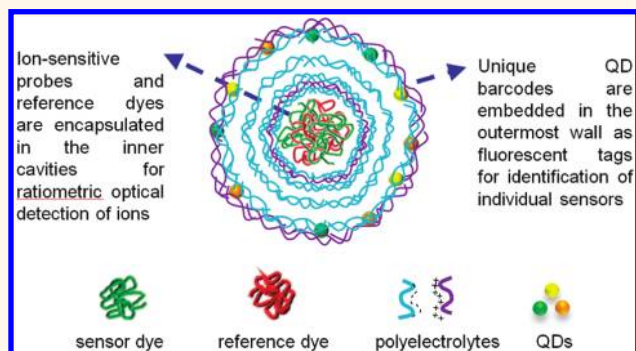
# Multiplexed Sensing of Ions with Barcoded Polyelectrolyte Capsules

Loretta L. del Mercato,<sup>†,‡,⊥</sup> Azhar Z. Abbasi,<sup>†,§,⊥</sup> Markus Ochs,<sup>†</sup> and Wolfgang J. Parak<sup>†,\*</sup>

<sup>†</sup>Fachbereich Physik and WZMW, Philipps Universität Marburg, Marburg, Germany <sup>‡</sup>Current address: National Nanotechnology Laboratory, Institute Nanoscience-CNR, Lecce, Italy. <sup>§</sup>Current address: Leslie Dan Faculty of Pharmacy, University of Toronto, Toronto ON, Canada. <sup>⊥</sup>These authors contributed equally to this work.

One technical desire in the sensing of ions is the quantitative detection of as many ionic species as possible in parallel. Depending on the applied method (*i.e.*, electrochemical or optical sensing) different problems for such multiplexed detection exist.<sup>1–5</sup> In the case of ion-sensitive fluorophores the major problem is spectral overlap between the emission spectra of the different fluorophores (*i.e.*, emission crosstalk).<sup>6,7</sup> Though a few fluorophores can be well distinguished there is a fundamental problem associated with the finite spectral width of wavelengths of fluorescent light where nearly all fluorescent dyes emit (from blue(violet) to NIR), which ultimately results in emission crosstalk. One suggested possibility of circumventing this problem is basing discrimination on spatial or temporal instead of spectral resolution.<sup>8</sup> The concept of spatial discrimination of different ion-sensitive fluorophores is straightforward. In case each different ion-sensitive fluorophore can be provided with a unique tag (which might be a fluorophore), and in case the average distance between different fluorophores is higher than the optical resolution limit, individual fluorophores can be separately addressed and read-out. Microcapsules built by layer-by-layer assembly are a promising system in this direction.<sup>9,10</sup> Such capsules (which basically have the geometry of a ping pong ball with porous walls) comprise a cavity, which can be loaded with ion-sensitive fluorophores, and a semipermeable wall formed out of several layers of polyelectrolytes, which can be tagged with a label to identify individual capsules.<sup>11</sup> By offering two separate spatial entities (cavity and wall) two different fluorescence sources (ion-sensitive fluorophore, fluorescence tag) can be integrated into one carrier system. Ion sensing with ion-sensitive probes integrated into particulate carrier systems has been demonstrated before.<sup>3,12,13</sup> Such integration of organic ion-sensitive fluorophores into

## ABSTRACT



Multiplexed detection of analytes is a challenge for numerous medical and biochemical applications. Many fluorescent particulate devices are being developed as ratiometric optical sensors to measure the concentration of intracellular analytes. The response of these sensors is based on changes of the emission intensity of analyte-sensitive probes, entrapped into the carrier system, which depends on the concentration of a specific analyte. However, there are a series of technical limits that prevent their use for quantitative detection of several analytes in parallel (*e.g.*, emission crosstalk between different sensor molecules). Here we demonstrate that double-wall barcoded sensor capsules can be used for multiplexed analysis of proton, sodium, and potassium ions. The sensor detection methodology is based on porous microcapsules which carry ion-sensitive probes in their inner cavity for ion detection and a unique QD barcode in their outermost wall as tag for identification of individual sensors. The engineering of QD barcodes to capsules walls represents a promising strategy for optical multianalyte determination.

**KEYWORDS:** polyelectrolyte capsules · quantum dots · barcode · ion sensing · fluorescence

particulate carrier systems offers several advantages. First, as several fluorophores are integrated *per* particle the absolute fluorescence intensity raises. Second, due to the particulate nature, individual particles (even at high concentration) can be identified in case their size is above the optical resolution limit. To assemble microcapsules for multiplexed ion-sensing we intended to make capsules filled with different ion-sensitive fluorophores in their cavities<sup>14</sup> which possess individual fluorescence tags

\* Address correspondence to wolfgang.parak@physik.uni-marburg.

Received for review August 15, 2011 and accepted November 4, 2011.

Published online November 04, 2011 10.1021/nn203344w

© 2011 American Chemical Society

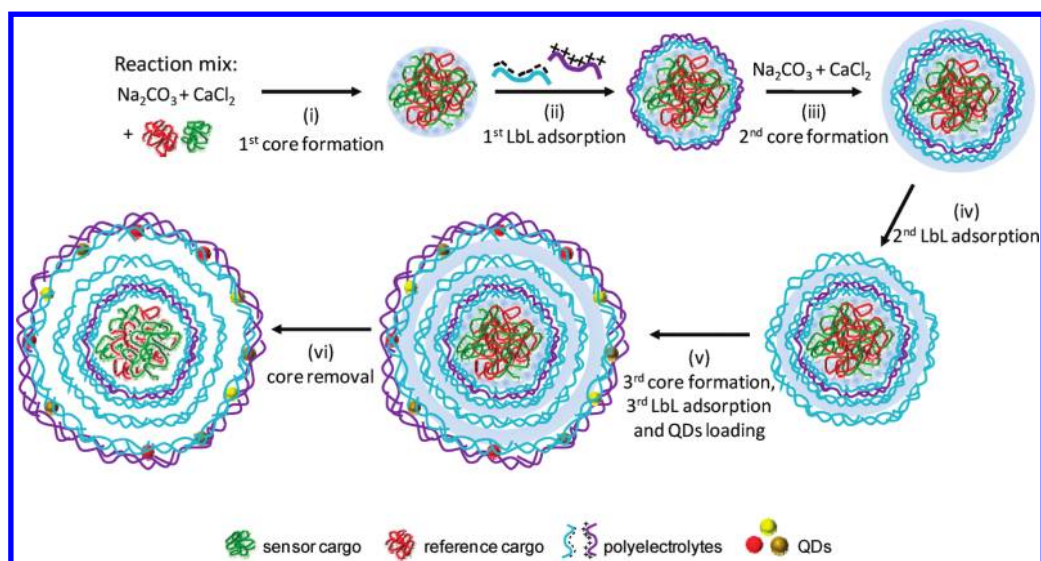
in their walls as tag for identification. High quantity tagging with fluorescent barcodes has been recently demonstrated with DNA-mediated assembly strategies of fluorophores<sup>5,15</sup> or quantum dots (QDs).<sup>16–19</sup> In our work, we fabricated microcapsules sensitive for  $H^+$ ,  $Na^+$ , and  $K^+$  (embedded with dextran conjugated with the ion-sensitive fluorophores FITC (fluorescein 5(6)-isothiocyanate), SBFI (sodium-binding benzofuran isophthalate), and PBFI (potassium-binding benzofuran isophthalate), respectively) (see Supporting Information, sections I, II). As tag we employed a simple digital QD barcode in the wall of the capsules (“0” or “1”) formed by the combination of three different QD colors (emission at 577, 596, and 610 nm), providing the principle capability for encoding seven different types of ion-sensitive microcapsules (“001”, “010”, “011”, “100”, “101”, “110”, “111”) (see Supporting Information, section IV). QDs were preferred to conventional organic fluorophores commonly used for fluorescence imaging for several reasons. First, they are characterized by a broad excitation spectrum and a narrow and more sharply defined emission peak.<sup>20</sup> Thus, a single light source can be used to excite multicolor QDs simultaneously without signal overlap.<sup>20,21</sup> Second, the fluorescence decay time for QDs is about 10–40 ns, which is longer than the fluorescence decay time of a few nanoseconds of typical organic fluorophores.<sup>20–22</sup> Third, QDs as prepared in our study, are charged and thus can be easily embedded within the charged shell of double-wall sensor capsules by employing the electrostatic forces that guide the LbL assembly of polyelectrolytes.<sup>11</sup> Lastly, QDs show minimal sensitivity to ions which is a crucial requirement for their use as fluorescent tags of the double-wall sensor capsules presented in this study. For tagging  $H^+$ ,  $Na^+$ , and  $K^+$  sensitive capsules the codes 001, 100, and 010 leading to orange, green, and yellow false-color, respectively, were employed. However, partial diffusion of dextran conjugated to the ion-sensitive fluorophores from the cavity to the wall of the capsules was observed.<sup>14</sup> Such phenomenon turned out to be a major problem when using capsules with QD barcode integrated in the walls. Indeed, the spatial separation of the fluorescence originating from the ion-sensitive fluorophores and the fluorescent QD barcode was hindered by the partial diffusion of labeled dextran to the walls. To circumvent this problem, capsules with two different walls were assembled by using a modified synthesis protocol previously reported by Kreft *et al.* (Scheme 1).<sup>23</sup> Such microcapsules comprise a cavity which can be filled with ion-sensitive fluorophores, which is surrounded by a first wall formed by multiple polyelectrolyte layers. A second polyelectrolyte wall with the integrated QD barcode is formed around the first one, whereby both walls are clearly spaced.<sup>23</sup> In this way ion-sensitive fluorophores in the cavity (and partly in the first wall) and QD barcodes in the second wall are spatially

separated (Scheme 1). As a result, capsules sensitive for  $H^+$ ,  $Na^+$ , and  $K^+$  can be identified by their fluorescent barcode in the outer walls and the  $H^+$ ,  $Na^+$ , and  $K^+$  concentrations can be determined by reading out the fluorescence intensity of the respective ion-sensitive fluorophores embedded in the capsule cavities.

## RESULTS AND DISCUSSION

In our work we employed the four different fluorophores FITC, SBFI, PBFI, and Dy647 (see Supporting Information, section II). While the blue-green fluorescence of FITC, SBFI, and PBFI is intentionally responsive to the concentration of  $H^+$ ,  $Na^+$ , and  $K^+$  ions in solution, Dy647 was chosen, as its red fluorescence in first order does not depend on the concentration of these ions. Consequently, in the case where FITC, SBFI, and PBFI are mixed with Dy647, ratiometric measurements of  $H^+$ ,  $Na^+$ , and  $K^+$  are possible, in which the ratio of the ion sensitive blue-green fluorescence is related to the constant red fluorescence. The fluorescence emission intensity of the four dyes under different  $H^+$ ,  $Na^+$ , and  $K^+$  ion concentrations is shown in Figure 1A. Data clearly indicate limited selectivity of the fluorophores used in this work. Besides  $Na^+$  and  $K^+$ , SBFI and PBFI also respond to  $H^+$  and PBFI also to  $Na^+$ , respectively, though with low sensitivity. However, sensitivity of the fluorophores was retained after their conjugation to dextran, as well as after encapsulation of the dye–dextran conjugates (Figure 1B) (see also Supporting Information, section III). As previously reported,<sup>14</sup> in the case of SBFI and PBFI sensor capsules, a charge effect of the amino-dextran on the fluorescence response of the indicators dyes occurs after their conjugation to charged dextran. It has been observed that positively charged amino-dextran affects the sensing properties of SBFI and PBFI by repelling sodium and potassium ions in the local environment. Consequently, the intensity of the fluorescence signal of dye–dextran conjugates is reduced compared to the one of free dyes. Nevertheless, an increase of the fluorescence signal of both the encapsulated SBFI–dextran and PBFI–dextran was detected at high  $Na^+$  and  $K^+$  concentrations (Figure 1B), thus indicating the ability of the capsules to sense low, medium, and high concentrations of these ions in the surrounding bulk solution.

To demonstrate multiplexed measurements, capsules loaded with dextran conjugated to FITC, SBFI, and PBFI (in addition to dextran conjugated to Dy647) in their cavity, and with orange, green, and yellow QD barcodes in their outer walls, respectively, were mixed and added to eight different solutions (Figure 2A) (see also Supporting Information, section V). The solutions were permutations of low/high  $H^+$  ( $c(H^+) = \text{pH } 9/\text{pH } 5$ ), low/high  $Na^+$  ( $c(Na^+) = 5 \text{ mM}/140 \text{ mM}$ ), and low/high  $K^+$  ( $c(K^+) = 5 \text{ mM}/140 \text{ mM}$ ). Fluorescence images were obtained by recording the fluorescence signals of the fluorophores loaded into the inner cavities



**Scheme 1.** LbL assembly of a multilayer polyelectrolyte double-wall sensor capsule. (i)  $\text{CaCO}_3$  microparticles are fabricated by coprecipitation from supersaturated  $\text{CaCl}_2$  and  $\text{Na}_2\text{CO}_3$  solutions mixed in the presence of the fluorescent analyte-indicator and the reference fluorophore covalently linked onto individual dextran polymers. (ii) Five bilayers of oppositely charged polyelectrolytes are consecutively adsorbed around the spherical templates by electrostatic attractions. (iii) The resulting core-shell particles are subjected to a second coprecipitation step leading to the formation of a second  $\text{CaCO}_3$  compartment. (iv) One layer of negatively charged polyelectrolyte is adsorbed around the resulting particles. Step v includes the synthesis of a third  $\text{CaCO}_3$  compartment accompanied by LbL absorption of five additional bilayers of (PSS/PAH) and one layer of QDs. Finally, a terminal polyelectrolyte PSS/PAH bilayer is added to terminate the LbL coating. The resulting particles are characterized by the following architecture:  $\text{CaCO}_3$ -dextran-fluorophores(PSS/PAH)<sub>5</sub>( $\text{CaCO}_3$ /PSS/ $\text{CaCO}_3$ )(PSS/PAH)<sub>4</sub>(QDs/PSS/PAH). (vi) All  $\text{CaCO}_3$  compartments are removed by dissolution with EDTA in order to obtain multilayer capsules with double cavities and double shells. In such a configuration, the sensor and reference fluorophores conjugated to dextran molecules are encapsulated within the inner cavity, whereas the QDs tags are embedded in the outermost shell. The two empty cavities serve as spacers which physically and optically separate the fluorescence signals of the sensor and reference fluorophores from the fluorescence signal of the QDs. This region avoids overlay of fluorescence signals and therefore the cross-talk between them.

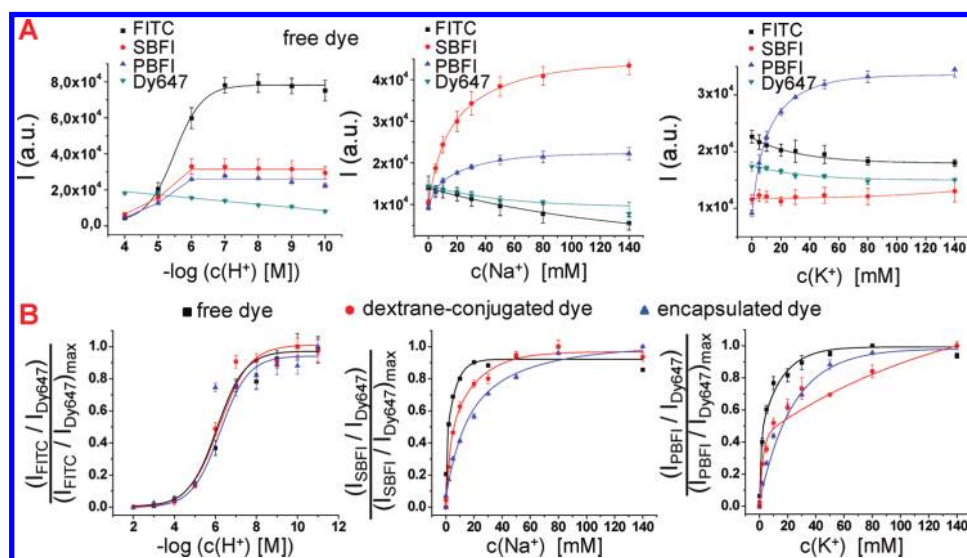


**Figure 1.** Fluorescence emission intensity of four different analyte sensitive fluorophores under different ion concentrations. (A) The fluorescence intensity ( $I$ ) of FITC, SBFI, PBFI, and Dy647 dyes is plotted versus pH ( $-\log(c(\text{H}^+))$ ), sodium ion concentration ( $c(\text{Na}^+)$ ), and potassium ion concentration ( $c(\text{K}^+)$ ). (B) The fluorescence response to ions is compared between the free organic dyes, the dyes conjugated to dextran, and dyes conjugated to dextran followed by encapsulation in a polyelectrolyte cavity. For ratiometric detection the ratios of fluorescence read-out of the ion-sensitive fluorophores FITC, SBFI, and PBFI ( $I_{\text{FITC}}$ ,  $I_{\text{SBFI}}$ ,  $I_{\text{PBFI}}$ ) and the nonsensitive reference fluorophore Dy647 ( $I_{\text{Dy647}}$ ) are determined and are normalized to the maximum ratios. These graphs represent the response curves of the ratiometric read-out to the presence of ions.

and the QDs embedded into the outermost shell. To achieve this accomplishment we used three distinct

excitation wavelengths ranges for the QDs barcodes, red reference dye, and ion-sensitive dyes. In particular,

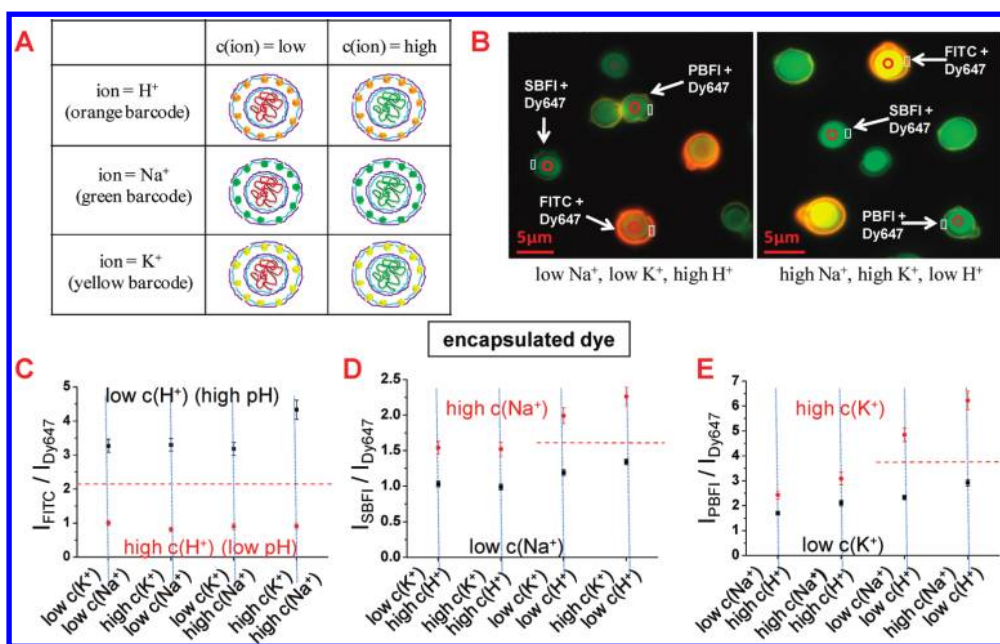


**Figure 2.** Multiplexed measurements of ions with barcoded polyelectrolyte sensor capsules. (A) Three different types of capsules have been synthesized. Capsules coloaded in their cavities with dextran modified FITC, SBFI, and PBFI and with dextran modified Dy647, which are thus sensitive to pH,  $\text{Na}^+$ , and  $\text{K}^+$ , respectively. These capsules were labeled with a quantum dot based orange, green, and yellow fluorescent barcode on their outermost surface, respectively. (B) Fluorescence image of a mixture of the three different types of capsules in two solutions with different ion concentrations; via the fluorescent barcode the type of each capsule can be clearly identified. By changing from a low  $\text{Na}^+$  ( $c(\text{Na}^+) = 5 \text{ mM}$ ,  $c(\text{K}^+) = 5 \text{ mM}$ ,  $\text{pH} = 5$ ) to a high  $\text{Na}^+$  condition ( $c(\text{Na}^+) = 140 \text{ mM}$ ,  $c(\text{K}^+) = 140 \text{ mM}$ ,  $\text{pH} = 9$ ) the  $I_{\text{SBFI}}/I_{\text{Dy647}}$  ratio of the sodium responsive capsules is raised, and in the false color fluorescence image the capsule cavities appear more blue-green compared to the more reddish appearance at low sodium concentration. (C–E) By variation of the pH from low (5) to high (9), the sodium concentration from low (5 mM) to high (140 mM), and the potassium concentration from low (5 mM) to high (140 mM) eight different combinations of ion concentrations with defined ion mixtures were generated. From left to right: The  $I_{\text{FITC}}/I_{\text{Dy647}}$ ,  $I_{\text{SBFI}}/I_{\text{Dy647}}$ , and  $I_{\text{PBFI}}/I_{\text{Dy647}}$  read-outs of the different capsules in these buffers were determined and are plotted here (data points represent mean values as determined from 30 capsules and standard deviations). The  $I_{\text{FITC}}/I_{\text{Dy647}}$  read-out of the pH-sensitive capsules clearly allows for distinguishing between low and high pH in all solutions, regardless the  $\text{Na}^+$  and  $\text{K}^+$  concentration. The red dotted line shows the threshold for the  $I_{\text{FITC}}/I_{\text{Dy647}}$  read-out distinguishing between low and high pH. The  $I_{\text{SBFI}}/I_{\text{Dy647}}$  and  $I_{\text{PBFI}}/I_{\text{Dy647}}$  read-outs of  $\text{Na}^+$  and  $\text{K}^+$  sensitive capsules allowed for distinguishing between low and high  $\text{Na}^+$  and  $\text{K}^+$  concentrations at high pH, and a threshold (red dotted line) can be given. At low pH SBFI as well as PBFI interfere with pH.

the ion-sensitive dyes were excited by using an excitation filter starting from 314 up to 366 nm, the yellow ( $\lambda_{\text{max,em}} = 577 \text{ nm}$ ), orange ( $\lambda_{\text{max,em}} = 595 \text{ nm}$ ) and red ( $\lambda_{\text{max,em}} = 615 \text{ nm}$ ) QDs were excited by using a single excitation filter starting from 485 up to 545 nm, and the red reference dye was excited by using an excitation filter starting from 620 up to 690 nm. A detailed description of the filter sets used for fluorescence imaging is provided in the Supporting Information (see section III.2). As can be seen from Figure 2B, the three different types of capsules can be clearly distinguished by their QD barcode in the outer wall (Figure 2B shows the overlay of all five channels). FITC-sensors are tagged with red barcode (001, shown in orange false colors), SBFI-sensors with green barcode (100, shown in green false colors) and PBFI-sensors with yellow barcode (010, shown in yellow false colors). Capsules are marked with small rectangular regions of interest (ROIs) in the QDs labeled walls and with spherical ROIs in the inner cavities. The calculated mean intensity values are yielded by the program for both kinds of ROIs and are entered into a calculation table (a detailed

description of the ratiometric analysis is provided in the Supporting Information, section IV). Since the capsules with orange, green, and yellow barcodes are filled with FITC, SBFI, and PBFI, plus Dy647, the blue-green to red ratio of the fluorescence originating from the capsules cavity is a measure for the surrounding  $\text{H}^+$ ,  $\text{Na}^+$ , and  $\text{K}^+$  concentration, respectively. Figure 2 panels B and C indicate that FITC filled capsules allow for clearly distinguishing with high precision between low and high  $\text{H}^+$  concentrations ( $\text{pH} = 5$ ,  $\text{pH} = 9$ ), regardless of the  $\text{Na}^+$  and  $\text{K}^+$  concentration. In the case of SBFI and PBFI filled capsules there is crosstalk with pH. In the case of high pH ( $\text{pH} = 9$ ) SBFI and PBFI loaded capsules can distinguish between low and high  $\text{Na}^+$  and  $\text{K}^+$  concentration (5 mM/140 mM), despite the respective  $\text{K}^+$  and  $\text{Na}^+$  concentration (Figure 2D,E). In other words, errors due to crosstalk between  $\text{Na}^+$  and  $\text{K}^+$  are significantly lower than the signal to be detected, which allows for discrimination of  $\text{Na}^+$  and  $\text{K}^+$  in parallel. This clearly demonstrated the possibility of multiplexed measurements. At high pH  $\text{H}^+$ ,  $\text{Na}^+$ , and  $\text{K}^+$  can be detected in parallel. In case the FITC read-out

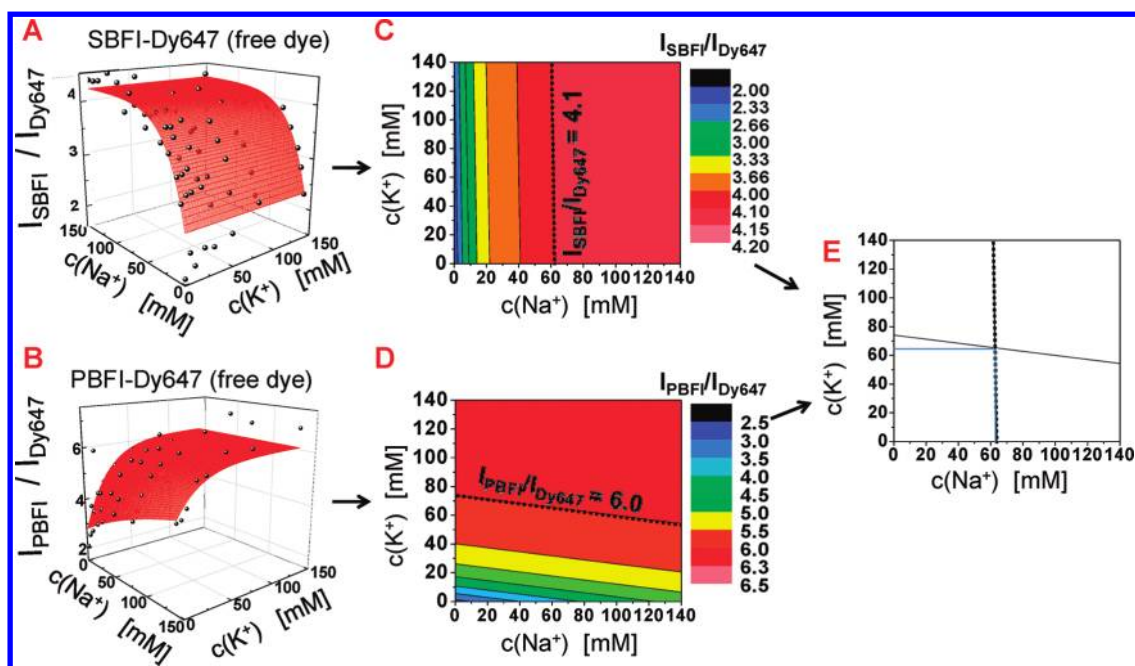


Figure 3. Cross-talk between sodium and potassium sensitive fluorophores in solutions with different ion concentrations. (A, B) Solutions with different sodium and potassium concentrations ( $c(\text{Na}^+)$ ,  $c(\text{K}^+)$ ) were prepared, and each one was split in two fractions. To one fraction a combination of SBFI and Dy647, to the other a combination of PBFI and Dy647 was given, always in the form of free dye molecules. The intensity of fluorescence of each dye was determined. (A) For the first fraction of each sample the ratio of SBFI to Dy647 emission ( $I_{\text{SBFI}}/I_{\text{Dy647}}$ ) was determined; (B) for the second fraction the ratio of PBFI to Dy647 emission ( $I_{\text{PBFI}}/I_{\text{Dy647}}$ ) was determined and plotted versus the  $\text{Na}^+$  and  $\text{K}^+$  concentration in a 3-dimensional representation. (C,D) A contour plot of the same data is represented, in which one looks toward the plane spanned by the  $c(\text{Na}^+)$  and  $c(\text{K}^+)$  axes and in which the intensity information ( $I_{\text{SBFI}}/I_{\text{Dy647}}$  and  $I_{\text{PBFI}}/I_{\text{Dy647}}$ ) is color coded. Lines and areas of equal color here correspond to concentration combinations of  $c(\text{Na}^+)$  and  $c(\text{K}^+)$  which have the same fluorescence read-out. If SBFI and PBFI emission corresponded only to changes in sodium and potassium concentration the lines of equal color in the  $I_{\text{SBFI}}$  and  $I_{\text{PBFI}}$  plots should be perpendicular to the  $c(\text{Na}^+)$  axis and to the  $c(\text{K}^+)$  axis, respectively. However, as the lines are slightly declined the SBFI and PBFI dye emission also responds to  $\text{K}^+$  and  $\text{Na}^+$  concentration, respectively. A situation is indicated in which the read-out of  $I_{\text{SBFI}}/I_{\text{Dy647}}$  was 4.1 and the read-out of  $I_{\text{PBFI}}/I_{\text{Dy647}}$  was 6.0. This represents two read-outs ( $I_{\text{SBFI}}/I_{\text{Dy647}}$  and  $I_{\text{PBFI}}/I_{\text{Dy647}}$ ) and two unknowns ( $c(\text{Na}^+)$ ,  $c(\text{K}^+)$ ). (E) By combining both read-outs in one graph the cross-section of the lines of equal  $I_{\text{SBFI}}/I_{\text{Dy647}}$  and equal  $I_{\text{PBFI}}/I_{\text{Dy647}}$  ratios lead to the concentration of sodium and potassium of the solution in which these read-outs have been determined.

indicates high pH the read-outs of SBFI and PBFI can be correlated to the  $\text{Na}^+$  and  $\text{K}^+$  concentration. In the case of low pH ( $\text{pH} = 5$ ) the read-out of SBFI and PBFI is corrupted by  $\text{H}^+$  (Figure 2D,E), which however is rather a problem of the used fluorophores and not an intrinsic problem of our detection scheme.

The proposed capsule sensor system should even help to reduce consequence of the cross-talk between different analyte sensitive fluorophores. Fluorescence of SBFI and PBFI primarily depends on  $\text{Na}^+$  and  $\text{K}^+$ , though there is crosstalk to  $\text{K}^+$  and  $\text{Na}^+$ , respectively.<sup>24</sup> In Figure 3 panels A and B, the response of both dyes in solutions with different  $\text{Na}^+$  and  $\text{K}^+$  concentrations is plotted. With the plain fluorophores one solution can either contain SBFI, or PBFI as ion-sensitive indicator, due to the high spectral overlap of both fluorophores. This is demonstrated in Figure 3 panels C and D. The blue-green to red ratio of the SBFI read-out provides one value, which however does not only depend on  $\text{Na}^+$ -concentration but also on  $\text{K}^+$ -concentration. In this way this value does not correspond to one point of concentration,  $c(\text{Na}^+)$ ,  $c(\text{K}^+)$ , but to a line. Small changes in the  $\text{Na}^+$  concentration can have

for example the same effect as big changes in the  $\text{K}^+$  concentration. If in case of SBFI the read-out corresponded only to  $\text{Na}^+$ , the line of equal SBFI read-out should be parallel to the  $c(\text{K}^+)$  axis (Figure 3C). The same is true for PBFI, which however is stronger influenced by crosstalk with  $\text{Na}^+$  then SBFI is influenced by crosstalk with  $\text{K}^+$  (Figure 3D). At any rate, read-out of only one fluorophore does not lead to unequivocally determined  $\text{Na}^+$  or  $\text{K}^+$  concentrations. However, by taking advantage of the geometry of the proposed capsule-based sensor system, both of SBFI and PBFI containing capsules can be placed in the same solution (as they can be spatially distinguished by their barcodes) for parallel detection of  $\text{Na}^+$  or  $\text{K}^+$  ions. Indeed, one can obtain two read-outs (SBFI and PBFI sensitive capsules) for two unknowns ( $\text{Na}^+$ ,  $\text{K}^+$  concentration). From each readout one obtains one line in the  $c(\text{Na}^+)$ – $c(\text{K}^+)$  plane, which corresponds to regions which fit to the determined blue-green-to-red ratio. However, as there are two lines their crossing point can be determined, which corresponds to one  $\text{Na}^+$  and one  $\text{K}^+$  concentration (Figure 3E) (see also Supporting Information, section VI). In this way, a

combination of several read-outs of cross talking fluorophores still allows for the determination of individual ion concentrations. It is important to point out that the key advantage of the capsule-based system is that it allows for reading out several analyte-sensitive fluorophores in parallel in the same solution. Clearly the performance of this system could be further improved in the future by using optimized analyte-sensitive fluorophores.

## CONCLUSIONS

The results show the possibility of measuring the concentration of several ions in parallel, indicating the

feasibility of the proposed sensors and the potential for their successful use in cells. Though fluorescence based sensing with particle based carriers has been described in the past,<sup>3,12</sup> we believe that the introduction of a QD barcode to capsules with two walls adds an important feature which allows for multiplexed measurements and thus for detecting several ions in parallel. Intracellular sensing in the lysosome for H<sup>+</sup> has been demonstrated with capsules.<sup>13</sup> Delivery of different types of capsules to the cytosol of cells and their multiplexed detection remains a challenge for the future.

## EXPERIMENTAL SECTION

**Fabrication of Double-Wall Barcoded Polyelectrolyte Capsules.** Calcium carbonate (CaCO<sub>3</sub>) porous microparticles with size distribution around 3.5–4 μm were obtained by mixing aqueous solutions of calcium chloride (CaCl<sub>2</sub>) (0.33 M) and sodium carbonate (Na<sub>2</sub>CO<sub>3</sub>) (0.33 M) in the presence of the fluorescent analyte-indicator (~50 μM) and the reference fluorophore (~50 μM) previously linked onto individual dextran polymers. Five bilayers of oppositely charged polystyrene sulfonate (PSS) and polyallylamine hydrochloride (PAH) polyelectrolytes were then consecutively adsorbed around the spherical templates by electrostatic attractions. The resulting core-shell particles were subjected to a second coprecipitation step. Then, one layer of PSS was adsorbed around the particle and a third coprecipitation step was performed before starting the third LbL assembly of four bilayers of (PSS/PAH). Subsequently, the coated particles were incubated in solutions of yellow (λ<sub>max,em</sub> = 577 nm), orange (λ<sub>max,em</sub> = 595 nm), and red (λ<sub>max,em</sub> = 615 nm) CdSe/ZnS quantum dots (QDs) with different concentrations. All QDs were coated with a amphiphilic polymer consisting of a polymer backbone [poly(isobutylene-alt-maleic anhydride)] to which alkylamine chains were linked *via* direct amidation between maleic anhydride and amino-ligands.<sup>25</sup> Finally, a terminal polyelectrolyte bilayer of (PSS/PAH) was added to complete the shell formation. The final structure of the double-wall sensor capsules was (PSS/PAH)<sub>5</sub>(CaCO<sub>3</sub>/PSS/CaCO<sub>3</sub>)(PSS/PAH)<sub>4</sub>(QDs/PSS/PAH). Finally, all CaCO<sub>3</sub> compartments were removed by dissolution with EDTA in order to obtain multilayer capsules with double cavities and double walls containing the fluorescent indicator and reference fluorophore within the inner cavity and QD barcode in the outermost wall. A detailed description of the synthesis is provided in the Supporting Information (see section I).

**QD Barcodes for Proton, Sodium, and Potassium Sensor Capsules.** The outermost wall of sensitive capsules for H<sup>+</sup>, Na<sup>+</sup>, and K<sup>+</sup>-ions was tagged with three different QD barcodes: 001, 100, and 010, leading to orange, green, and yellow false-colors, respectively. In particular, H<sup>+</sup>-sensitive capsules were tagged with code 001 obtained by mixing equal volumes of 0.01 μM yellow (λ<sub>max,em</sub> = 577 nm), 0.01 μM orange (λ<sub>max,em</sub> = 595 nm), and 0.1 μM red (λ<sub>max,em</sub> = 615 nm) QDs. Na<sup>+</sup>-sensitive capsules were tagged with code 100 obtained by mixing equal volumes of 0.1 μM yellow, 0.01 μM orange, and 0.01 μM red QDs. K<sup>+</sup>-sensitive capsules were tagged with code 010 obtained by mixing equal volumes of 0.01 μM yellow, 0.1 μM orange and 0.01 μM red QDs. The detailed description of the sample preparation and labeling methods are provided in the Supporting Information (see section IV).

**Multiplexed Measurements of Proton, Sodium, and Potassium Sensor Capsules.** The fluorescence behavior of double-wall sensor capsules sensitive for H<sup>+</sup>, Na<sup>+</sup> and K<sup>+</sup>-ions was investigated by mixing the three types of sensor capsules altogether in buffer solutions containing different ions in low or high concentration. The samples were analyzed *via* fluorescence microscopy after

5 min of equilibration time of the capsules in the aqueous ion solutions. In total, five channels were scanned independently to register all fluorescence signals: two channels for detecting the sensor and reference fluorophores loaded into the inner cavities and three channels for detecting the three QDs embedded into the outermost shell. The obtained fluorescent images were processed using the ImageJ v1.42 m software (<http://rsb.info.nih.gov/ij/>) in order to perform ratiometric analysis. Capsules were marked with ROIs of the same size and shape in the outer shell and in the inner cavity to read-out the fluorescence tag in the outermost shell as well as the fluorescence changes of the cavity. The program calculates for every marked capsule the barcode tag and thereby the type of capsule. Furthermore it shows the type of ion for which the fluorescence of the corresponding sphere is sensitive. Using the data from the cavities, the program calculates the average concentration (low or medium) of the corresponding ions in solution. The detailed description of sample preparation, fluorescence imaging, and data analysis are given in the Supporting Information (see sections III, IV, and V).

**Acknowledgment.** This work was supported by in part by BMBF/ERANET Nanosyn and EU Nandiatream (grants to W.J.P.). AZA is thankful to HEC (Pakistan)/DAAD for the fellowship.

**Supporting Information Available:** Description of capsule synthesis procedure and characterization *via* electron microscopy (SEM and TEM); description of the optical properties of ion-sensitive fluorophores and fluorescence measurements of their crosstalk; studies of the effect of encapsulation on the fluorophore signals *via* fluorescence spectrometer and fluorescence microscopy measurements; description of the barcode labeling approach; description of the multiplexed measurements and parallel determination of ions *via* fluorescence microscopy analysis. This material is available free of charge *via* the Internet at <http://pubs.acs.org>.

## REFERENCES AND NOTES

- Goodey, A.; Lavigne, J. J.; Savoy, S. M.; Rodriguez, M. D.; Currey, T.; Tsao, A.; Simmons, G.; Wright, J.; Yoo, S.-J.; Sohn, Y.; *et al.* Development of Multianalyte Sensor Arrays Composed of Chemically Derivatized Polymeric Microspheres Localized in Micromachined Cavities. *J. Am. Chem. Soc.* **2001**, *123*, 2559–2570.
- Bakker, E.; Bhakthavatsalam, V.; Gemene, K. L. Beyond Potentiometry: Robust Electrochemical Ion Sensor Concepts in View of Remote Chemical Sensing. *Talanta* **2008**, *75*, 629–635.
- Lee, Y. E. K.; Smith, R.; Kopelman, R. Nanoparticle Pebble Sensors in Live Cells and *in Vivo*. *Annu. Rev. Anal. Chem.* **2009**, *2*, 57–76.
- Medintz, I. L.; Uyeda, H. T.; Goldman, E. R.; Mattoussi, H. Quantum Dot Bioconjugates for Imaging, Labelling and Sensing. *Nat. Mater.* **2005**, *4*, 435–446.

- Li, Y. G.; Cu, Y. T. H.; Luo, D. Multiplexed Detection of Pathogen DNA with DNA-Based Fluorescence Nanobarcodes. *Nat. Biotechnol.* **2005**, *23*, 885–889.
- Ruedas-Rama, M. J.; Wang, X.; Hall, E. A. A Multi-ion Particle Sensor. *Chem. Commun. (Cambridge)* **2007**, 1544–1546.
- Choi, Y.; Park, Y.; Kang, T.; Lee, L. P. Selective and Sensitive Detection of Metal Ions by Plasmonic Resonance Energy Transfer-based Nanospectroscopy. *Nat. Nanotechnol.* **2009**, *4*, 742–746.
- Abbasi, A. Z.; Amin, F.; Niebling, T.; Friede, S.; Ochs, M.; Romero, S. C.; Martos, J. M. M.; Rivera Gil, P.; Heimbrod, W.; Parak, W. J. How Colloidal Nanoparticles Could Facilitate Multiplexed Measurements of Different Analytes with Analyte-Sensitive Organic Fluorophores. *ACS Nano* **2011**, *5*, 21–25.
- Decher, G. Fuzzy Nanoassemblies: Toward Layered Polymeric Multicomposites. *Science* **1997**, *277*, 1232–1237.
- Donath, E.; Sukhorukov, G. B.; Caruso, F.; Davis, S. A.; Möhwald, H. Novel Hollow Polymer Shells by Colloid-Templated Assembly of Polyelectrolytes. *Angew. Chem., Int. Ed.* **1998**, *37*, 2202–2205.
- Rivera Gil, P.; del Mercato, L. L.; del Pino, P.; Muñoz Javier, A.; Parak, W. J. Nanoparticle-Modified Polyelectrolyte Capsules. *Nano Today* **2008**, *3*, 12–21.
- Buck, S. M.; Koo, Y. L.; Park, E.; Xu, H.; Philbert, M. A.; Brausel, M. A.; Kopelman, R. Optochemical Nanosensor Pebbles: Photonic Explorers for Bioanalysis with Biologically Localized Embedding. *Curr. Opin. Chem. Biol.* **2004**, *8*, 540–546.
- Kreft, O.; Muñoz Javier, A.; Sukhorukov, G. B.; Parak, W. J. Polymer Microcapsules as Mobile Local pH-Sensors. *J. Mater. Chem.* **2007**, *17*, 4471–4476.
- del Mercato, L. L.; Abbasi, A. Z.; Parak, W. J. Synthesis and Characterization of Ratiometric Ion-Sensitive Polyelectrolyte Capsules. *Small* **2011**, *7*, 351–363.
- Um, S. H.; Lee, J. B.; Kwon, S. Y.; Li, Y.; Luo, D. Dendrimer-like DNA-Based Fluorescence Nanobarcodes. *Nat. Protoc.* **2006**, *1*, 995–1000.
- Han, M.; Gao, X.; Su, J. Z.; Nie, S. Quantum-Dot-Tagged Microbeads for Multiplexed Optical Coding of Biomolecules. *Nat. Biotechnol.* **2001**, *19*, 631–635.
- Sheng, W.; Kim, S.; Lee, J.; Kim, S. W.; Jensen, K.; Bawendi, M. G. *In-Situ* Encapsulation of Quantum Dots into Polymer Microspheres. *Langmuir* **2006**, *22*, 3782–3790.
- Lee, J. A.; Mardiyani, S.; Hung, A.; Rhee, A.; Klostranec, J.; Mu, Y.; Li, D.; Chan, W. C. W. Toward the Accurate Read-out of Quantum Dot Barcodes: Design of Deconvolution Algorithms and Assessment of Fluorescence Signals in Buffer. *Adv. Mater.* **2007**, *19*, 3113–3118.
- Fournier-Bidoz, S.; Jennings, Travis L.; Klostranec, Jesse M.; Fung, W.; Rhee, A.; Li, D.; Chan, Warren C. W. Facile and Rapid One-Step Mass Preparation of Quantum-Dot Barcodes. *Angew. Chem., Int. Ed.* **2008**, *47*, 5577–5581.
- Alivisatos, A.; Gu, W.; Larabell, C. Quantum Dots as Cellular Probes. *Annu. Rev. Biomed. Eng.* **2005**, *7*, 55–76.
- Chan, W. C. W.; Maxwell, D. J.; Gao, X.; Bailey, R. E.; Han, M.; Nie, S. Luminescent Quantum Dots for Multiplexed Biological Detection and Imaging. *Curr. Opin. Biotechnol.* **2002**, *13*, 40–46.
- Michalet, X.; Pinaud, F. F.; Bentolila, L. A.; Tsay, J. M.; Doose, S.; Li, J. J.; Sundaresan, G.; Wu, A. M.; Gambhir, S. S.; Weiss, S. Quantum Dots for Live Cells, *in Vivo* Imaging, and Diagnostics. *Science* **2005**, *307*, 538–544.
- Kreft, O.; Prevot, M.; Möhwald, H.; Sukhorukov, G. B. Shell-in-Shell Microcapsules: A Novel Tool for Integrated, Spatially Confined Enzymatic Reactions. *Angew. Chem., Int. Ed.* **2007**, *46*, 5605–5608.
- Meuwis, K.; Boens, N.; De Schryver, F. C.; Gallay, J.; Vincent, M. Photophysics of the Fluorescent  $K^+$  Indicator PBF1. *Biophys. J.* **1995**, *68*, 2469–2473.
- Lin, C.-A. J.; Sperling, R. A.; Li, J. K.; Yang, T.-Y.; Li, P.-Y.; Zanella, M.; Chang, W. H.; Parak, W. J. Design of an Amphiphilic Polymer for Nanoparticle Coating and Functionalization. *Small* **2008**, *4*, 334–341.